J Therm Anal Calorim (2012) 110:807–811
DOI 10.1007/s10973-011-1997-4

$\alpha \rightarrow \gamma$ Lithium borate phase transition produced during the CO_2 chemisorption process

Alfredo Román-Tejeda · Heriberto Pfeiffer

Received: 3 August 2011 / Accepted: 11 October 2011 / Published online: 2 November 2011

Abstract CO_2 capture and storage are the most important issues to be tackled in the near future. For the last few years, different lithium ceramics have been proposed as possible CO_2 captors. In this article, the CO_2 chemisorption process on α-$LiBO_2$, which had not been previously investigated, was studied. α-$LiBO_2$ was synthesized and characterized by XRD, SEM and N_2 adsorption. Its CO_2 reactivity was evaluated by dynamic and isothermal thermogravimetric experiments. Results show that α-$LiBO_2$ is able to react with CO_2. Additionally, there is a phase transformation from α-$LiBO_2$ to γ-$LiBO_2$ during the CO_2 absorption. Although the CO_2 absorption was not considerably high, the results showed that lithium ceramics, containing boron, absorbed CO_2.

Keywords Chemisorption · Carbon dioxide · Lithium borate · Phase transition

Introduction

There are many techniques and materials that could be used to reduce the levels of carbon dioxide in the atmosphere [1, 2]. Among the different materials used in this research field, different alkaline and earth-alkaline ceramics have been proposed as possible CO_2 captors because of the chemisorption process occurring between CO_2 and the alkaline or the earth-alkaline atoms present in the ceramic, such as Li_4SiO_4, Li_2ZrO_3, Na_2ZrO_3, Li_5AlO_4 and CaO [3–8]. Generally, all alkaline and earth-alkaline ceramics display similar chemisorption reaction mechanisms, where initially, the CO_2 is chemisorbed over the ceramic surface particles, producing an external shell of the alkaline or the earth-alkaline carbonate and the corresponding residual oxide. To continue the CO_2 chemisorption and complete the reaction in the ceramic bulk, the diffusion processes must be activated [9]. It has been previously found that diffusion processes are the limiting steps in the CO_2 absorption process [10]. It has been reported that the synthesis of different solid solutions, such as $Li_{2-x}Na_xZrO_3$ [11] and $Li_{4-x}Na_xSiO_4$ [12], improves not only the kinetic parameters but also the efficiency and the absorption temperature range, among other properties of the CO_2 absorption reaction. In fact, some of the improvements observed in the solid solutions have been attributed to punctual modifications in the crystalline structure of the ceramics. Therefore, the addition of small and light elements, such as boron, may modify the crystalline structure of the lithium ceramics locally, producing new and interesting results.

Conversely, lithium borates have been used for different electrical and optical applications, as well as for glass structural components [13, 14]. Among the lithium borates, there are two $LiBO_2$ phases: the α-$LiBO_2$ and the γ-$LiBO_2$. The α-$LiBO_2$ system has an anhydrous monoclinic phase that is stable at high temperatures. This α-$LiBO_2$ phase possesses an endless laminar chain structure of $[BO_3]^{1-}$ triangles with Li–O bonds between the chains [15]. The lattice parameters of this phase are $a = 5.838$ Å, $b = 4.348$ Å, $c = 6.449$ Å and $\beta = 115.121°$ [16]. On the contrary, the γ-$LiBO_2$ phase is quenchable, and it has a tetragonal structure with the following lattice parameters $a = 4.1961$ Å and $c = 6.5112$ Å [16]. When subjected to a pressure of 3.5 GPa at 850 °C, the α-$LiBO_2$ undergoes a

A. Román-Tejeda · H. Pfeiffer (✉)
Instituto de Investigaciones en Materiales, Universidad Nacional Autónoma de México, Circuito exterior s/n CU, Del. Coyoacán, 04510 México, DF, Mexico
e-mail: pfeiffer@iim.unam.mx

transformation from tri-coordinated ($^{[3]}$B) to tetra-coordinated boron ($^{[4]}$B), forming dense tetrahedral γ-$LiBO_2$ [15].

In previously reported cases, the lithium and sodium ceramics with layered structures have presented good properties such as high temperature CO_2 captors [17]. Therefore, the aim of the present work was to determine whether the α-$LiBO_2$ phase was able to capture CO_2. This finding will be useful in further studies in which boron may be used to prepare solid solutions with other lithium ceramics, among other possible applications.

Experimental section

Initially, α-$LiBO_2$ was synthesized dissolving lithium carbonate (Li_2CO_3, Aldrich) and boric acid (H_3BO_3, Sigma) in water. Subsequently, the solution was heated at 60 °C with continuous stirring till it was dry. Finally, the powders produced were pulverized and heat-treated at 700 °C for 8 h. To obtain the α-$LiBO_2$ phase, different Li/B molar ratios were tested because boron tends to produce liquid phases, which segregate and produce diverse boron oxides at high temperatures [18].

Firstly, the characterization was performed on the initial α-$LiBO_2$ phase by using X-ray diffraction (XRD). Once the existence of the α-$LiBO_2$ phase was corroborated, it was further characterized and evaluated by scanning electron microscopy (SEM), textural analysis (N_2 adsorption), thermogravimetric (TG) analysis and infrared spectroscopy (FTIR). XRD analyses were performed in a Bruker AXS D8 ADVANCE diffractometer using $CuK_{\alpha 1}$ radiation. Subsequently, the particle size and the morphology of the α-$LiBO_2$ material were studied using a scanning electron microscope (Stereoscan 440, Cambridge-Leica). Being a non-conductive sample, the powder was initially covered with gold. Finally, the surface area of the material was determined by the N_2 adsorption–desorption isotherm, which was obtained with a Minisorp II (Bel-Japan). The BET surface area was calculated from the N_2 adsorption isotherm. The sample was previously degasified at room temperature for 12 h under vacuum.

The CO_2 capture capacity was tested in a Q500HR thermobalance (TA Instruments), with a CO_2 flow rate of 60 mL/min. Different dynamic and isothermal experiments were performed. Additionally, a differential scanning calorimetry (DSC) experiment was performed using the DSC equipment from Instruments Specialists Incorporated. The DSC sample was heated in a CO_2 atmosphere from room temperature to 600 °C at a rate of 10 °C/min. Finally, some of the CO_2 isothermal samples were further analyzed by TG and by FTIR spectroscopy. The latter was performed using a NICOLET 6700 FT-IR Spectrometer.

Results and discussion

α-$LiBO_2$ was synthesized by varying the Li/B molar ratio from 1:1 to 1:2. When the stoichiometric Li/B molar ratio of 1:1 was used, a mixture of amorphous and crystalline phases was obtained. The detected crystalline phases corresponded mainly to lithium phases such as LiOH, Li_2CO_3 and Li_2O. These results strongly suggest that the boron fused, thereby producing the amorphous phase, which inhibited the α-$LiBO_2$ production. This result agrees with the phase diagram reported by Sastry [18]. Therefore, to synthesize α-$LiBO_2$, the Li/B molar ratio was varied. The XRD pattern of the $LiBO_2$ sample with a Li/B molar ratio of 2:1 is shown in Fig. 1A. This pattern fitted to the 84-0118 JCPDS file, which corresponds to α-$LiBO_2$. No other compounds were identified, which indicates that the sample is pure, at least at the XRD detection level. It should be noted that after the heat treatment, two different segregated materials were obtained: (1) A white powder was obtained, which corresponded to the α-$LiBO_2$ phase, according to the XRD results, and (2) a glass was produced and pasted on the bottom of the crucible, which must correspond to a boron amorphous oxide produced from the

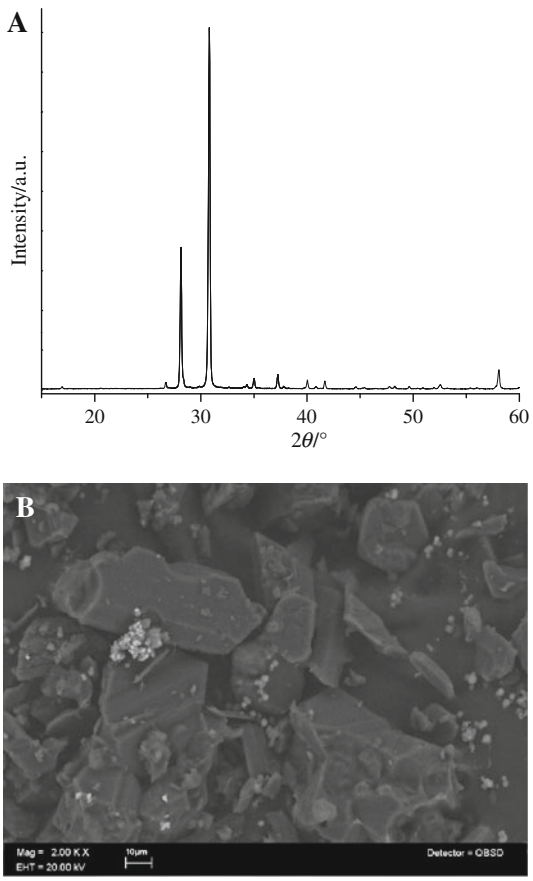

Fig. 1 XRD pattern (**A**) and BSE image (**B**) of the α-$LiBO_2$ sample

excess boron. Additionally, as the final powder had to be scratched and pulverized, some preferential orientation was observed on the XRD pattern in the form of a considerably high-intensity 002 peak ($2\theta = 30.6^{\circ}$).

Figure 1B shows the morphology of the α-$LiBO_2$ particles. The particles are polyhedral in shape with a large particle size distribution ranging between 30 and 60 μm. The surface area of the particles was determined by the N_2 adsorption–desorption isotherm using the BET method (S_{BET}). The S_{BET} value obtained was 1.3 m^2/g. The morphology, the particle size and the surface area fit very well with the synthesis method (solid-state reaction) used here, and these values are similar to those obtained for other lithium ceramics that have been tested as CO_2 captors.

If the α-$LiBO_2$ phase were able to absorb CO_2, the reaction proposed should be the following one:

$$2\ LiBO_2 + CO_2 \rightarrow Li_2CO_3 + B_2O_3 \quad (1)$$

In such a case, the maximum CO_2 chemisorption capacity of this ceramic would be 10.04 $mmol/g_{ceram}$. Although two moles of $LiBO_2$ are necessary to absorb 1 mol of CO_2, the material would be theoretically able to chemisorb similar CO_2 quantities to those presented by other lithium ceramics [6, 17, 19, 20]. Here, $LiBO_2$ presents an advantage in boron, which is a very light element in comparison with the previously mentioned elements (copper and zirconium) that are used as structural ceramics.

Figure 2 shows a α-$LiBO_2$ dynamic thermogram acquired in a CO_2 atmosphere. Firstly, the sample showed an increment of 0.7% in the mass of the α-$LiBO_2$ between room temperature and 385 °C. This increment of mass may be attributed to the CO_2 absorption over the surface of the α-$LiBO_2$ particles. The main CO_2 chemisorption process was further carried between 385 and 488 °C, where the sample absorbed 2.8 wt%. Although it is evident that an important CO_2 desorption process is activated at temperatures higher than 480 °C, the thermogram shows a constant increment in mass up to 700 °C, indicating that the CO_2 absorption continues. It must be noted from the thermogram that the maximum CO_2 absorption temperature is 488 °C, which is lower than the temperatures observed for other lithium ceramics. Most often, the lithium ceramics show a maximum CO_2 absorption at temperatures ≥550 °C.

To analyze the CO_2 absorption on α-$LiBO_2$ further, different isothermal studies were performed (Fig. 3). The isothermal experiment performed at 400 °C presents a typical exponential behavior, increasing the mass to 1.4 wt% after 4 h. The isotherms obtained between 420 and 460 °C present similar trends, showing an increase in the CO_2 absorption as a function of increasing temperature from 1.9 wt% to 2.7 wt%. The isotherms recorded at 480 °C and higher temperatures show a decrease in the

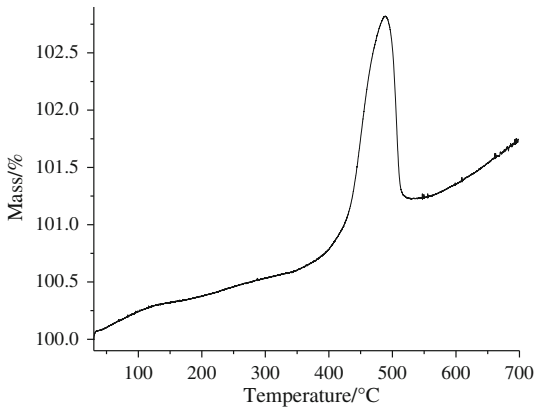

Fig. 2 Dynamic thermogravimetric analysis of the α-$LiBO_2$ into a flux of CO_2

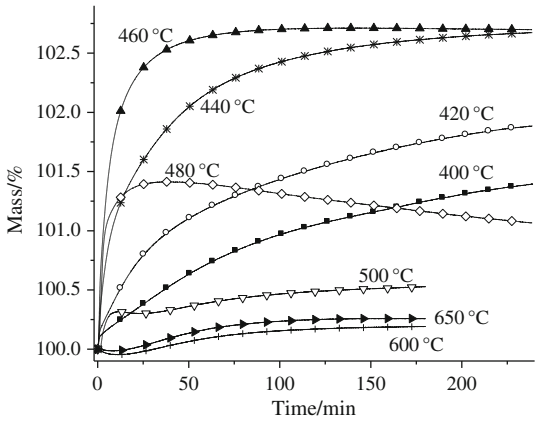

Fig. 3 Isothermal thermogravimetric analyses of CO_2 chemisorption on α-$LiBO_2$ at different temperatures

CO_2 absorption. For short durations, these isotherms seem to absorb CO_2, following a similar trend to that observed in the previous isotherms. However, at longer durations, the isotherm presented a loss in the mass, which implies that the CO_2 desorption has already been activated.

To corroborate the chemical trapping of the CO_2 by the α-$LiBO_2$, some of the isothermally treated samples were characterized by TG and FTIR. Figure 4 presents the thermograms of the α-$LiBO_2$, both as prepared and after the isothermal CO_2 absorption at 440 °C. Both experiments were performed in an open air atmosphere. The original α-$LiBO_2$ sample showed a small but continuous mass loss of 0.25% between 120 and 400 °C, which can be attributed to different processes: dehydration of crystalline water, surface dehydroxylation and decarbonation processes [15, 21]. On the contrary, after the isothermal CO_2 absorption at 440 °C, the sample only presented a well-defined mass loss, centered at 420 °C, which confirmed the absorption of CO_2 onto the ceramic. The mass loss (2.5%) is very similar to the mass increment produced during the isothermal

experiment (2.2%). In this case, the decarbonation process was produced at lower temperatures compared to the initial CO_2 dynamic thermogram (Fig. 2). This can be explained by taking into account that, in the first case, the atmosphere was CO_2, which must have resulted in shifting the desorption equilibrium to higher temperatures.

Figure 5 shows the FTIR spectra of the α-$LiBO_2$ original sample and of the other samples after the isothermal CO_2 absorption. The α-$LiBO_2$ original sample presents an identical spectrum to the one previously reported for this phase [15]. The broad absorption bands between 1100 and 1450 cm^{-1} are attributed to the B–O stretching vibrations of the BO_3 species, whereas the vibration bands present between 800 and 1100 cm^{-1} are attributed to the B–O bond stretching of tetrahedral BO_4 units. Finally, the integrated vibration peaks of BO_3, BO_4 and Li–O are located between 400 and 800 cm^{-1} [14, 15, 22–24]. Once the ceramic was carbonated, either at 420 or 460 °C, the initial FTIR bands corresponding to the α-$LiBO_2$ phase disappeared, and new and stronger band vibrations appeared. These new band vibrations were located at 459, 681, 758, 828 and 960 cm^{-1}, where all of them fitted very well to the vibration bands of the γ-$LiBO_2$ phase [15]. These changes indicate a phase transformation from α-$LiBO_2$ to γ-$LiBO_2$, which occurred during the isothermal carbonation. Only the band vibration located at 828 cm^{-1} was broader and with a higher intensity compared to the previous literature reports, which can be explained by the vibration band of Li_2CO_3, which occurs at a similar position, 840–860 cm^{-1} [25]. Finally, FTIR spectra of the samples, thermally treated at 500, 600 and 650 °C, showed that α-$LiBO_2$ phase was almost totally recovered.

To support these results, a DSC experiment was performed. Figure 6 shows the results from a DSC experiment performed on the α-$LiBO_2$ sample in a CO_2 atmosphere. This curve shows three different endothermic peaks at 392, 467 and 496 °C. The first two endothermic peaks can be associated with the CO_2 absorption and the α → γ $LiBO_2$ phase transformation, respectively, while the third signal may be attributed to the CO_2 desorption and/or the γ → α −$LiBO_2$ phase transformation processes, according to the TG and FTIR results. In fact, the first and the third DSC endothermic peaks agree with the CO_2 absorption temperature range observed in the TG analysis, as shown in the Fig. 2. Therefore, the second endothermic peak observed at 467 °C must correspond to the α → γ $LiBO_2$ phase transformation, as previously indicated by the FTIR analysis.

Certain features from the previous FTIR and DSC results should be noted. α-$LiBO_2$ is transformed into the γ-$LiBO_2$ phase during the thermal carbonation process. However, this phase transition reversed when the process was performed at 500 °C or higher temperatures. Of course, a part of the ceramic reacted to produce lithium carbonate. These findings are all in good agreement with the literature, where it has been shown that α-$LiBO_2$

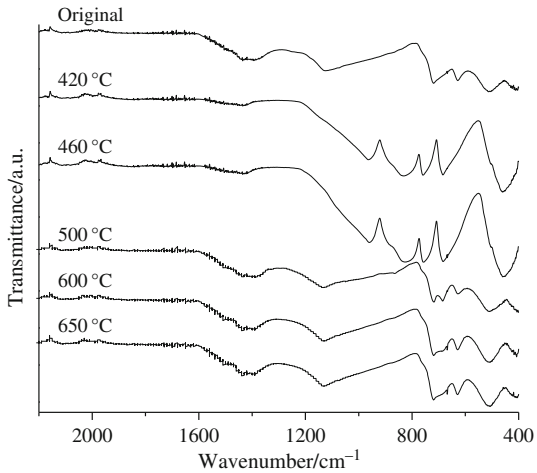

Fig. 5 FTIR spectra of the α-$LiBO_2$ sample, after the isothermal CO_2 absorption at different temperatures and as prepared

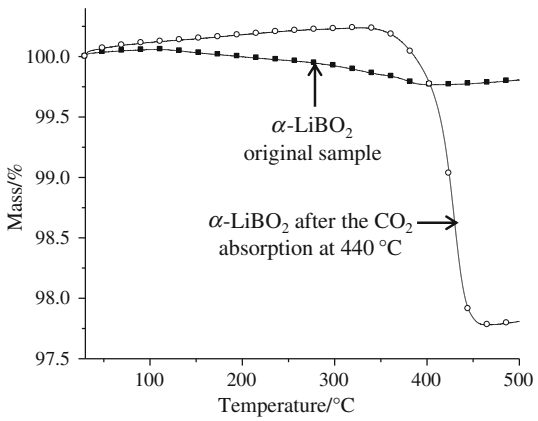

Fig. 4 Dynamic thermogravimetric analyses of the α-$LiBO_2$ original sample and the sample treated isothermically at 440 °C under a CO_2 atmosphere

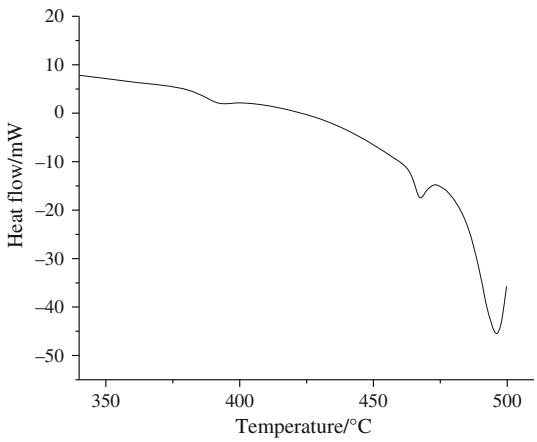

Fig. 6 DSC analysis of the α-$LiBO_2$ sample into a CO_2 atmosphere

transforms into γ-$LiBO_2$ at both increasing temperature (850 °C) and pressure (3.5 GPa) [15]. Additionally, Liang et al. [21] reported the α → γ phase transition under isothermal heating at T ≤ 570 °C and atmospheric pressure, but starting the transition from the amorphous phase rather than the crystalline $LiBO_2$ phase. These reports strongly suggest that the CO_2 absorption mainly occurs over the γ-$LiBO_2$ phase. Initially, the α-$LiBO_2$ phase begins to absorb CO_2 between the room temperature and approximately 400 °C. Subsequently, the α → γ $LiBO_2$ phase transformation occurs, which enhances the CO_2 absorption significantly. Finally, once the α-$LiBO_2$ phase is recovered from the γ → α phase transformation, the CO_2 absorption is strongly reduced. This behavior may be explained by the phase structure because the γ-$LiBO_2$ phase is denser than the α-$LiBO_2$ phase [15]. Hence, the phase transformation may be the limiting step of the CO_2 capture process.

Conclusions

α-$LiBO_2$ was synthesized and characterized. It presented a dense polyhedral morphology with a small surface area, 1.3 m^2/g. The thermal analysis performed in a CO_2 flow, along with the DSC and FTIR studies, showed that the α-$LiBO_2$ was transformed into the γ-$LiBO_2$, characterized by a mass gain, indicating that the γ-$LiBO_2$ phase was responsible for the CO_2 capture process. Boron, being a very light element in comparison with the other structural elements, may be useful in the production of solid solutions, where it may help to modify and increase the CO_2 absorption properties of ceramics.

Acknowledgements This study was financially supported by ICyT-DF (179/2009) and PAPIIT-UNAM (IN100609). Authors thank to A. Tejeda, M. Canseco and O. Novelo for technical help.

References

1. Zhao HY, Cao Y, Lineberry Q, Pan WP. Evaluation of CO_2 adsorption capacity of solid sorbents. J Therm Anal Calor. 2011;106:199–205.
2. Barbosa MN, Araujo AS, Galão LPFC, Silva EFB, Santos AGD, Luz-Jr. GE, Fernandes-Jr. VJ. Carbon dioxide adsorption over DIPA functionalized MCM-41 and SBA-15 molecular sieves. J Therm Anal Calor (2011). doi:10.1007/s10973-011-1398-8.
3. Nakagawa K, Ohashi T. A novel method of CO_2 capture from high temperature gases. J Electrochem Soc. 1998;145:1344–6.
4. Choi KH, Korai Y, Mochida I. Preparation of CO_2 absorbent by spray pyrolysis. Chem Lett. 2003;32:924–5.
5. Xiong R, Ida JI, Lin YS. Kinetics of carbon dioxide sorption on potassium-doped lithium zirconate. Chem Eng Sci. 2003;58:4377–85.
6. Veliz-Enriquez MY, Gonzalez G, Pfeiffer H. Synthesis and CO_2 capture evaluation of $Li_{2-x}K_xZrO_3$ solid solutions and crystal structure of a new lithium-potassium zirconate phase. J Solid State Chem. 2007;180:2485–92.
7. Pfeiffer H, Vazquez C, Lara VH, Bosch P. Thermal behavior and CO_2 absorption of $Li_{2-x}Na_xZrO_3$ solid solutions. Chem Mater. 2007;419:922–6.
8. Ida JI, Xiong R, Lin YS. Synthesis and CO_2 sorption properties of pure and modified lithium zirconate. Sep Purif Technol. 2004;36:41–51.
9. Mosqueda H, Vazquez C, Bosch P, Pfeiffer H. Chemical sorption of carbon dioxide (CO_2) on lithium oxide (Li_2O). Chem Mater. 2006;18:2307–10.
10. Pannocchia G, Puccini M, Seggiani M, Vitolo S. Experimental and modeling studies on high-temperature capture of CO_2 using lithium zirconate based sorbents. Ind Eng Chem Res. 2007;46:6696–706.
11. Pfeiffer H, Lima E, Bosch P. Lithium-sodium metazirconate solid solutions, $Li_{2-x}Na_xZrO_3$ ($0 \leq x \leq 2$): A hierarchical architecture. Chem Mater. 2006;18:2642–7.
12. Mejía-Trejo VL, Fregoso-Israel E, Pfeiffer H. Textural, structural and CO_2 chemisorption effects produced on the lithium orthosilicate by its doping with sodium ($Li_{4-x}Na_xSiO_4$). Chem Mater. 2008;20:7171–6.
13. Kodama M, Kojima S. Anharmonicity and fragility in lithium borate glasses. J Therm Anal Calor. 2002;69:961–70.
14. Dang-Huy N, Badilescu S, Djaoued Y, Girouard F, Bader G, Ashrit PV, Vo-Tan T. Preparation and characterization of lithium metaborate thin films obtained by a sol-gel method. Thin Solid Films. 1996;286:141–5.
15. Lei L, He D, He K, Qin J, Wang S. Pressure-induced coordination changes in $LiBO_2$. J Solid State Chem. 2009;182:3041–8.
16. Zachariasen WH. The crystal structure of lithium metaborate. Acta Crystal. 1964;17:749–51.
17. Palacios-Romero L, Lima E, Peiffer H. Structural analysis and CO_2 chemisorption study on non-stoichiometric lithium cuprates ($Li_{2+x}CuO_{2+x/2}$). J Phys Chem A. 2008;113:193–8.
18. Sastry BS, Hummel FA. Studies in lithium oxide systems: V, Li_2O–Li_2O B_2O_3. J Am Ceram Soc. 1959;42:216–8.
19. Choi S, Drese JH, Jones CW. Adsorbent materials for carbon dioxide capture from large anthropogenic point sources. ChemSusChem. 2009;2:796–854.
20. Alcerreca-Corte I, Fregoso-Israel E, Pfeiffer H. CO_2 absorption on Na_2ZrO_3: a kinetic analysis of the chemisorption and diffusion processes. J Phys Chem C. 2008;112:6520–5.
21. Liang J, Chen X, Min J, Chai Z, Zhao S, Cheng X, Zhang Y, Rao G. Crystallization mechanism of dehydrated amorphous $LiBO_2$. Phys Rev B. 1995;51:756–62.
22. Kamitsos EI, Karakassides MA, Chryssikos GD. Vibrational spectra of magnesium-sodium-borate glasses. 2. Raman and mid-infrared investigation of the network structure. J Phys Chem. 1987;91:1073–9.
23. Chryssikos GD, Kamitsos EI, Patsis AP, Bitsis MS, Karakassides MA. The devitrification of lithium metaborate: polymorphism and glass formation. J Non-Cryst Solids. 1990;126:42–51.
24. Almeida AFL, Vasconcelos IF, Valente MA, Sombra ASB. The optical and ^{57}Fe Mössbauer spectra of lithium diborate ($Li_2B_4O_7$) in borophosphate glass-ceramics. Physica B. 2002;322:276–88.
25. Zhang DR, Liu HL, Jin RH, Zhang NZ, Liu YX, Kang YS. Synthesis and characterization of nanocrystalline $LiTiO_2$ using a one-step hydrothermal method. J Ind Eng Chem. 2007;13:92–6.